A Novel Method of Fault Location for Single-Phase Microgrids

Jiajun Duan, *Student Member, IEEE*, Kaifeng Zhang, *Member, IEEE*, and Liang Cheng, *Member, IEEE*

***Abstract*—This paper presents a novel fault location method for single-phase microgrids. In order to locate a fault, a feature specific to the fault location is found, namely the maximum oscillation magnitude of the transient voltage signal induced by the fault. Our theoretical study and extensive simulations demonstrate that there is an approximated linear relationship between the maximum magnitude of the transient signal observed by a sensor, and the distance between the sensor and the fault location. Based on the discovered relationship, microgrid topology and sensor location information, we have designed an algorithm capable of locating the fault in the single-phase microgrids. The proposed fault location method has been implemented and validated through simulations in Electro-Magnetic Transients Program and MATLAB. The average localization error is less than 10% in the evaluation results, which manifests the significance of the novel method, as there is little research done for fault location in single-phase microgrids.**

***Index Terms*—Distributed generators (DGs), fault location, single-phase microgrid, transient signal.**

I. Introduction

MICROGRID is "a group of interconnected loads and distributed energy resources within clearly defined electrical boundaries that acts as a single controllable entity with respect to the grid" [1]. According to the U.S. Department of Energy, microgrid has drawn increasing attention in recent years because it has many advantages such as utilizing green energy resources, offering flexible operations, and promoting reliability and resilience when utility grids experience disturbances [2].

Based on the number of grid phases, microgrids can be categorized as three- and single-phase systems. Three-phase microgrids have been studied by many researchers and installed in utility power grids [3]. Meanwhile, single-phase microgrids are applicable to power systems with relatively small power and low-voltage levels, such as residential house, small commercial lot, ship, space station, minor military base, or island scenarios [4], [5].

This paper focuses on solving the problem of fault location in single-phase microgrids. In each hierarchy of power grid, from transmission, distribution to microgrid, fault location is an important problem. Thus a good amount of fault location methods have been studied by researchers.

Automatic fault location in microgrids is necessary in many situations [17], [23] where identifying the fault location is required to be done in a short period of time for maintenance efficiency and operation cost saving, such as in ship, space station, military base, island, and mission-critical scenarios, or when the lines are buried underground or implanted in the structure that makes visually inspecting lines cost-prohibitive if not impossible.

A. Related Work

Fault location in transmission networks generally assumes a long transmission line with sensors deployed at either one or both ends of the line. The travelling wave (TW) method utilizes the time difference between the incidence wave and the reflection wave of transient voltage/current signals caused by disturbance to identify the fault location [6], [7]. The TW method is also the key method suggested by the IEEE guide for fault location on ac transmission and distribution lines [8]. Jafarian and Sanaye-Pasand [6] proposed a solution to detect small-voltage-magnitude faults that happen very close to the sensors or when a single phase is grounded.

Fault location in distribution networks is usually accomplished based on the information collected by one main sensor. Distribution networks often have relatively smaller scales and more complicated topologies compared to transmission networks. The typical topology of distribution networks is a tree with the main sensor installed at the root of the tree, namely the distribution substation. The wavelet transform (WT) method in [9] is introduced to find the fault branch. Its theoretical foundation depends on the high frequency components of transient signals which may have different performances with respect to the different paths they pass through. Based on this idea, Borghetti *et al.* [10] considered that there is a characteristic frequency corresponding to a certain location of distribution networks. The fault location can be determined by comparing the theoretical frequency with the frequency identified by the WT. However, the characteristic frequency is related to many other factors in practice

Manuscript received October 3, 2014; revised December 25, 2014, April 18, 2015, and August 3, 2015; accepted September 15, 2015. Date of publication October 8, 2015; date of current version February 17, 2016. This work was supported by the U.S. Department of Energy under Grant DE-OE0000428. Paper no. TSG-00983-2014.

J. Duan is with the Department of Electrical Engineering, Lehigh University, Bethlehem, PA 18015 USA (e-mail: jid213@lehigh.edu).

K. Zhang is with the Department of Computer Science and Engineering, Lehigh University, Bethlehem, PA 18015 USA, on leave from the School of Automation, Southeast University, Nanjing 210096, China (e-mail: kaifengzhang@seu.edu.cn).

L. Cheng is with the Department of Computer Science and Engineering, and the Laboratory of Networking Group (LONGLAB), Lehigh University, Bethlehem, PA 18015 USA (e-mail: cheng@cse.lehigh.edu).

Color versions of one or more of the figures in this paper are available online at http://ieeexplore.ieee.org.

Digital Object Identifier 10.1109/TSG.2015.2480065

which can be easily disturbed. In [11], high frequency components ($10^3 - 10^9$ Hz) are first extracted by the WT. Then the fault distance is calculated by the TW method which increases the noise immunity. There still exist other methods (see [12]), which require a precise simulation to calculate the fault location.

One of the main problems when trying to use aforementioned methods in a microgrid is that these methods need data acquisition devices with fairly high sampling rates to achieve the high resolution in fault location needed for the microgrid. For example, in the traveling wave approach [9], it needs to detect the time difference between the first transient wave and the second transient wave arriving at the sensor; in the transmission line case the time difference is in a magnitude of seconds corresponding to a wave traveling distance of about 100 km while in a microgrid the time difference would be in a magnitude of $10^{-6}-10^{-7}$ s if such concept would still apply. Thus, as further explained in Section II-B, it is infeasible to perform accurate fault location for typical microgrid deployment based on the traveling wave approach. Related research for three-phase microgrids only addresses fault detection problems. The difference between fault location and fault detection is that solving the fault location problem needs to identify the accurate location of the fault while solving the fault detection problem only needs to detect whether a fault has happened on certain line or not. For instance, new methods of fault detection for three-phase microgrids include frequency shift [13], phase shift [14], high impedance detection [15], and harmonic current injection [16]. These methods take three-phase symmetric components as their basic features and are capable of working in both transmission networks and distribution networks. Other fault detection methods use data mining and *d–q* WT approach, respectively [17], [18], which are both specifically designed for three-phase microgrids. These methods can only achieve the wide area protection while the realization of accurate fault location in microgrids is still absent.

B. Uniqueness and Contribution of Our Research

To the best of our knowledge, no research about automatic and accurate fault location in single-phase microgrids has been done up till now. The difference between single-phase microgrids and transmission, distribution and three-phase microgrids makes this paper full of challenges.

1) Three-phase related features such as unbalance attribute components are no longer available and this leads us to search for new features that may be used for fault location in single-phase microgrids.
2) The traveling wave approaches used in transmission and distribution networks would require a sampling rate of an analog to digital conversion in dozens of gigabit per second to extract the feature of traveling waves in microgrids, which would not be feasible in a typical microgrid deployment. A detailed analysis is described in Section II-B.

It is unknown whether the existing research ideas for fault detection in three-phase microgrids discussed above could be easily applied to the fault location problem in single-phase microgrids or not because there is no existing research that addresses this open question.

Therefore, in our research, we explore various features available in single-phase microgrids and investigate their relationship with the fault patterns. Through extensive simulations we have discovered a new feature and its relationship with fault location and designed a novel approach for solving the fault location problem for single-phase microgrids based on information fusion from multiple sensors. We have validated the approach with theoretical and simulation studies. The major contributions of this paper include the following.

1) Revealing the approximated linear relation between the magnitude of transient signals and the fault distance in single-phase microgrids. When a short-circuit fault occurs, voltage sensors should detect an oscillating transient signal. The longer the distance between the sensor and the fault location, the larger the magnitude of the transient signals sensed.
2) Designing an appropriate algorithm for fault location based on the newly discovered relationship and evaluating the performance of the algorithm including its error analysis and robustness analysis. The average localization error is less than 10% in the evaluation results, which manifests the significance of the novel method as there is little research done for fault location in single-phase microgrids.

The remainder of this paper is structured as follows. Section II presents the fault location problem and introduces the proposed approach. Section III establishes the theoretical foundation of the novel approach. Section IV describes the designed algorithm; in order to demonstrate the correctness of the algorithm. Section V presents the simulation design of four cases and their results including error analysis and robustness evaluation of the algorithm. Finally, Section VI concludes this paper.

II. Problem Statement and Proposed Approach

A. Problem Statement

Without loss of generality, in order to satisfy microgrid stability requirements such as those prescribed by IEEE1547, we assume that a microgrid has a control center or a centralized supervisory control and data acquisition/energy management system that collects sensor data and adjust operation states of the microgrid [19]. Generally, the protective relays are installed at distributed generators (DGs) and important loads and there is no protection device for each transmission line in such microgrids. Therefore, it may be labor-intensive and time-consuming to locate a fault that has happened in a transmission line spanning hundreds of meters that may be hard to inspect. As shown in Fig. 1, we also assume that each DG in the microgrid has a data acquisition device, and there is also a data acquisition device installed at the interface between the microgrid and the external grid. In Fig. 1, dotted lines denote information flows sent from sensors to the central controller and dashed lines represent the control signal flows from the central controller to the DGs. Each circuit line is marked as T_i. As mentioned in [20], centralized control performs well in

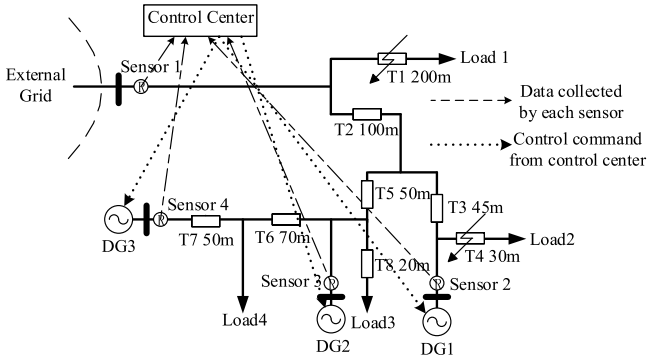

Fig. 1. Microgrid with centralized control.

microgrids and is not difficult to realize while there also exist microgrids adopting decentralized control. In this paper, we focus on microgrids with centralized control and the decentralized control scenarios will be our future research work.

In general, for the problem of fault location in single-phase microgrids, the following prerequisites are used.

1) The microgrid topology is known.
2) The basic system parameters are known. For instance, the accurate line length and approximately the equivalent impedances of circuits.
3) The basic circuit principles and theorems are applicable, such as Ohm's law, Kirchhoff's law, and Thevenin's theorem.
4) The electrical signals can be sampled by multiple sensors in the microgrid at the same time.

The fault location problem in single-phase microgrids is to estimate the fault position based on the aforementioned information and the error between the estimated fault location and the actual fault location should be within an engineering tolerance margin. For example, assume that a short circuit has occurred at the midpoint of transmission line 4 (T4) in the microgrid shown in Fig. 1. The transient voltage signal caused by the short circuit has been sensed by sensors 1–4. Using the sensor data along with the known topology and system parameter information, a fault location solution should be able to estimate that the fault has happened at somewhere close to the midpoint of T4. The error between the estimated fault location and the actual fault location should be within an engineering tolerance margin.

B. Revisiting Fault Location Methods for Different Domains

A single-phase microgrid may only run across several hundred meters, which results in discrepancies between microgrids and other networks in terms of phase features, network complexity, geographical coverage, and system parameters.

The fault location problem of a transmission network concerns about a group of long cables or overhead lines. In the transmission network, sensors are usually deployed at one or two sides of the transmission line. If there are sensors installed at both ends, a precise synchronism device is required to support the synchronized sampling function. The long length of a transmission line provides comparatively accurate circuit parameters and also warrants a recognizable resolution of signal features to be extracted.

Because of these differences, fault location methods in transmission networks cannot be directly applied in the microgrid. The features used in those methods overlap due to microgrid's short electrical distance. For example, the TW method [9] calculates the fault location via the time difference between the first transient wave and the second transient wave arriving at the sensor using the following formula:

$$t = 2 \cdot (L - l)/v \tag{1}$$

where L is the total transmission length, l is the distance between the fault location and the sensor, v is the propagation velocity of the transient wave which is close to the light velocity, namely $3 \cdot 10^8$ m/s. As the length of microgrid is generally about several hundred meters, the data acquisition devices would have to be able to discriminate two different features within $10^{-6} - 10^{-7}$ s should the above-mentioned approach based on (1) be applied. The sampling rate of an analog to digital conversion should be in dozens of gigabit per second to extract the feature, which would not be feasible in a typical microgrid deployment.

The fault location problem in a distribution network is often based on a tree or radial topology. The main monitoring devices are generally installed at the interface of the distribution substation because it depends on the single sensor to determine the fault location and fault type, the data acquisition devices need quite high sampling rate. To compare the current sampling information with existing information in the database is an effective way to identify fault location.

The fault location methods for distribution networks lose their effectiveness in single-phase microgrids too. The main reason is still the problem of features getting overlapped because of the short electrical distances and sensor limitations.

Therefore, the practical engineering requirements motivate us to develop a new fault location method which is specifically designed for the single-phase microgrids.

C. Proposed Approach

We believe that the essence in solving the fault location problem in single-phase microgrids is to find a feature which corresponds to the distance from the fault location to the sensor. Thus we conduct theoretical studies and simulation experiments seeking such features. The detailed theoretical derivation is presented in Section III.

The simulations of short circuit in single-phase microgrids are performed in the Electro-Magnetic Transients Program (EMTP). After analyzing data collected by each sensor deployed at every important node, we find that the basic electrical signals are impacted by the fault occurrence. The changes in current and frequency are difficult to distinguish. Nevertheless, the transient signals of voltage present an observable pattern with different fault locations.

Take the microgrid in Fig. 1 as an example. When a short circuit occurs at the transmission line 1 (T1), the entire and the zoomed-in view of transient voltage signals received by the four sensors during the fault period are plotted in Fig. 2(a) and (b). If the fault occurs at the transmission line 4 (T4), the entire and the zoomed-in view of transient voltage signals are plotted in

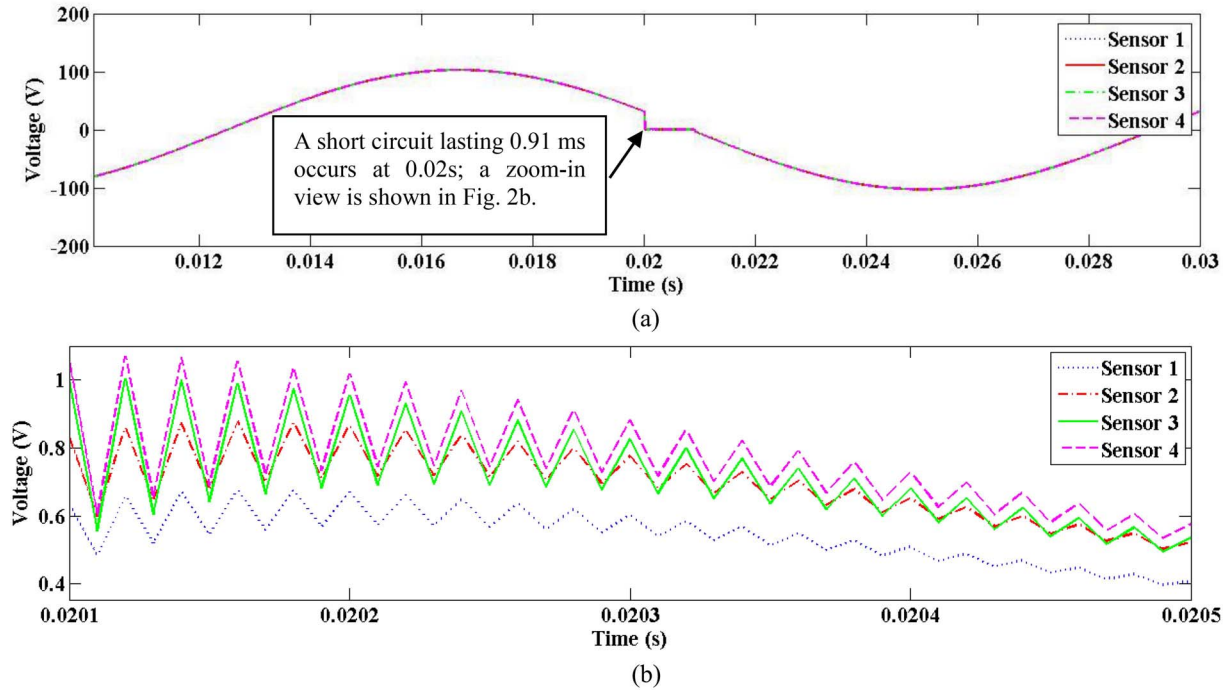

Fig. 2. (a) Transient voltage signals caused by a short circuit at T1 in a microgrid depicted as Fig. 1 during fault time. (b) Zoomed-in view of transient voltage signals caused by a short circuit at T1 in a microgrid depicted as Fig. 1 during fault time.

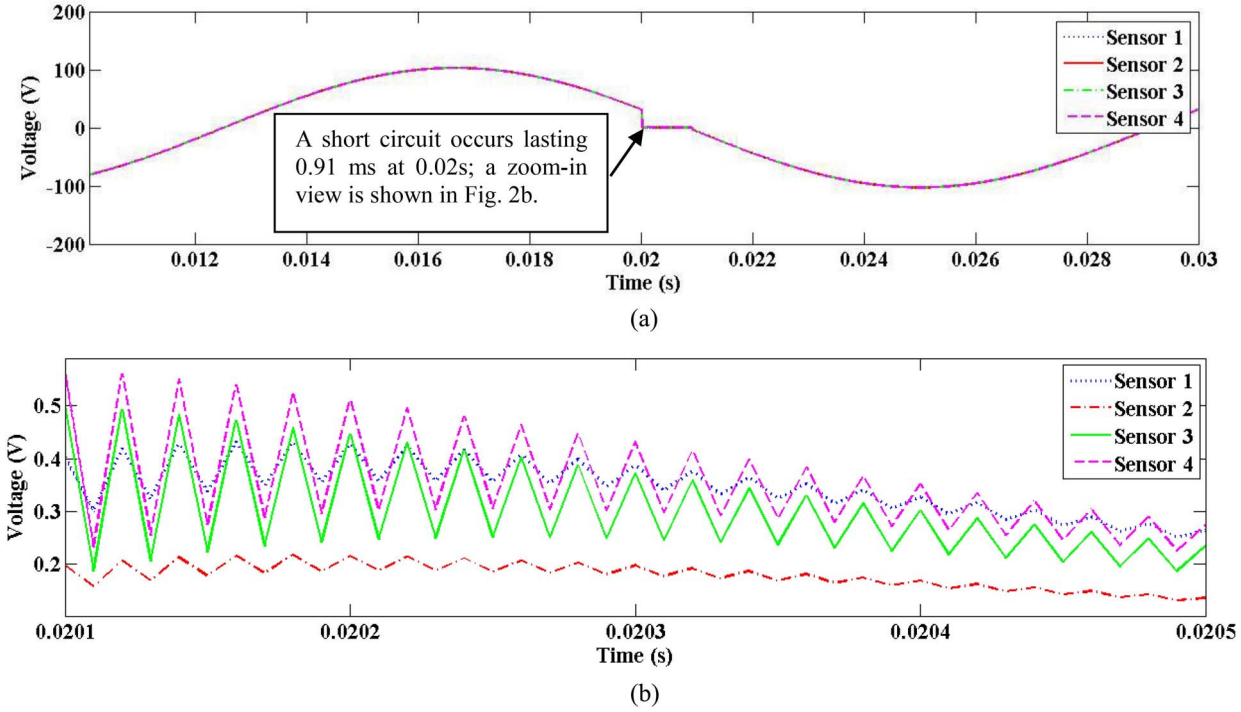

Fig. 3. (a) Transient voltage signals caused by a short circuit at T4 in a microgrid depicted as Fig. 1 during fault time. (b) Zoomed-in view of transient voltage signals caused by a short circuit at T4 in a microgrid depicted as Fig. 1 during fault time.

Fig. 3(a) and (b). The zoomed-in views cover the time period between 0.0201 and 0.0205 s for a clear and discernible visual effect of the transient signals from the sensors.

It can be seen that an abrupt change of voltage at the fault point results in oscillatin transient signal fluctuations. The closer a sensor sits from the fault location the smaller the magnitude of the transient signal it observes. In other words, the magnitude of the transient voltage signal becomes larger when the distance between the sensor and the fault location is longer.

Extensive simulation data presented in Section IV show that the maximum magnitude of transient signals is proportional to the distance between the fault and the sensor. Let y represent the maximum magnitude of transient signals, and x is the

distance between the fault location and the sensor. Then the relationship between y and x approximate a linear function

$$y = a \cdot x + b \tag{2}$$

where a and b are constant coefficients associated with each specific microgrid.

The general process of our fault location method can be summarized as follows.

1) The transient signals are detected by each sensor and the data are input to the algorithm.
2) Possible fault locations are estimated by the algorithm with known information, including the above-mentioned linear relationship, the microgrid topology, and the system parameters such as the length of each circuit.
3) The possible fault locations are ranked based on the comparison between the calculated magnitude of the transient signal and the actual magnitude observed by sensors.
4) The coefficients in the linear relationship are calibrated using the information of the actual fault location found based on the estimated fault location.

Besides the significance of the discovered relationship for the fault location method, another merit of our research is that it takes advantage of multisensor availability in a microgrid. The detailed method derivation, illustration, and validation are described in the following sections.

III. Theoretical Analysis

This section analyzes the principle supporting the discovered relationship mentioned above. The full-scale theoretical analysis of a typical microgrid as depicted in Fig. 1 is a daunting challenge. Thus we simplify the short circuit situation of the microgrid as an equivalent circuit shown in Fig. 4. Z_{ex} is the equivalent impedance of the external grid. Z_1 is the transmission line impedance in series with similar small short ground impedance which represents different short circuit distances. For example, assume that a short circuit occurs at T1 in Fig. 4. When observing from sensor 1, its left side is equivalent to a combination of input voltage and external impedance denoted as V_{in} and Z_{ex}. For its right side, the only remaining part after short-isolated is the impedance from the sensor to the fault location in series with short ground impedance marked as Z_1. The output voltage V_{out} is the voltage that applied on Z_1. Similarly, a one-port equivalent circuit of short line can be obtained from the port of any other sensors. In this paper, we use the simple switching transient analysis by Laplace transform for post-fault states [21] to illustrate that different fault positions will cause different transient behaviors. Note that the feature used in our approach is extracted during the post-fault stage where there is no topology change

$$H(s) = \frac{X_1}{X} + \left(\frac{R_1}{X} - \frac{R \cdot X_1}{X^2}\right) \Big/ \left(s + \frac{R}{X}\right) \tag{3}$$

$$H(t) = \frac{X_1}{X} \cdot \delta(t) + K \cdot e^{-\frac{R}{X}t} \tag{4}$$

where $X = X_1 + X_{\text{ex}}$, $R = R_1 + R_{\text{ex}}$, $K = (R_1/X) - (R \cdot X_1/X^2)$, and $\delta(t)$ is an impulse function. Generally in the low voltage level grids (e.g., below 110 kV), the resistance weighs more than the reactance. Thus, if the input voltage is a sinusoidal function of frequency, the output voltage is an oscillated attenuating signal. Fig. 5 presents examples of the transient voltage response when $R_1 = 0.04, 0.06, 0.08$, and 0.1 ohm, $X_1 = 10^{-4}$ ohm, $R_{\text{ex}} = 5$ ohm, and $X_{\text{ex}} = 0.4$ ohm. The influence of the resistance on the maximum magnitude of the oscillation signal is obvious: the larger the resistance, the larger the maximum magnitude.

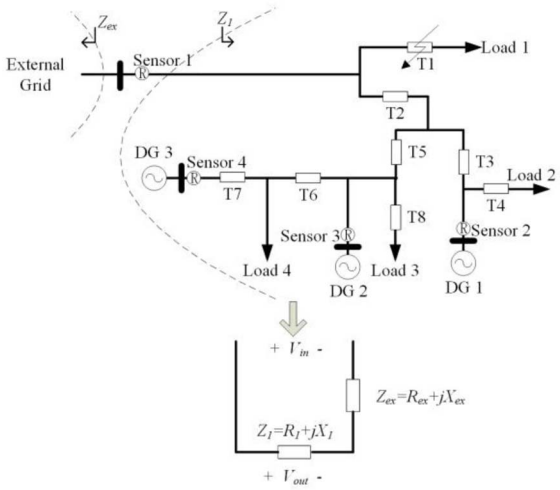

Fig. 4. Equivalent circuit of a microgrid with short circuit.

From the derivation shown above, it can be concluded that the magnitude of the transient response is proportional to R_1, i.e., proportional to the electrical distance if the circuit line is homogeneous. Therefore, the discovered relation between the magnitude of transient voltage signals and the distance between the sensor and the fault location has its theoretical support, which builds the foundation for the fault location algorithm design described in the next section.

IV. Algorithm Design

The major objective of running a fault location method is to provide fault position estimations for the microgrid maintenance staff to efficiently locate and eliminate the fault when it happens. In this paper, we differentiate two different types of fault position in the microgrid. One type is called an internal circuit fault (ICF) which has sensors deployed at both sides of the line where the fault occurs, e.g., T2 in Fig. 1. The other type is a called load side fault (LSF), meaning that a fault occurs at the load side, e.g., T1 in Fig. 1.

A. Fault Distance Calculation

After a fault occurs, the data collected by each sensor during the fault period will be acquired as the input to the algorithm. By analyzing transient signals collected by the sensors, the algorithm identifies the sensor that has observed the smallest magnitude of the transient signals as the closest one to the fault location. As shown in Fig. 6(a), if we assume that there are n sensors in a single-phase microgrid and the fault spot is x meters away from the closest sensor i, the distance between the fault location and any sensor j can be expressed

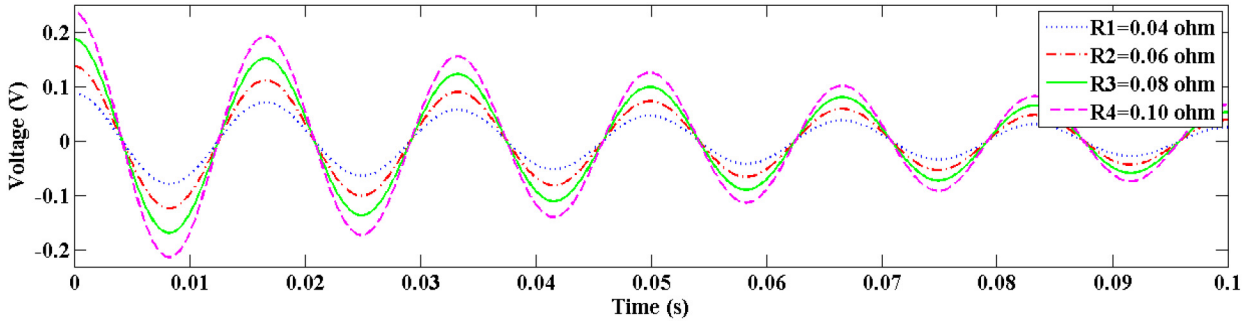

Fig. 5. Output waveform of the equivalent circuit.

using x and d_{ij}, i.e., the distances between sensors i and j, as $(d_{ij}+x)$ or $(d_{ij}-x)$; the plus or minus sign corresponds to the LSF or the ICF defined above. Thus the relationship between the maximum magnitude of the transient signals and the fault location can be expressed

$$\begin{cases} y_i = a \cdot x + b \\ y_j = a \cdot \left(d_{ij} \pm x\right) + b \end{cases} \quad [j \in n, j \neq i]. \tag{5}$$

We first assume that the fault is an ICF and use the minus sign to derive x. In fact, if there are more than two sensors in the microgrid, we may obtain an over-determined equation set as each sensor data can provide an equation based on (5). The method of left division may be used to find an approximate solution of x.

The calculated x only indicates an approximate location estimation if the fault is an LSF. That is why the algorithm needs to rank the possible fault locations estimated to offer more information to the microgrid maintenance staff.

B. Fault Location Ranking

Based on the calculated distance x between the fault location and the nearest sensor, we can generate a list of possible fault locations by finding the intersections of a circle centered at the sensor with a radius of x and the related circuit lines. For example, as shown in Fig. 6(a), the possible fault locations corresponding to the sensor 1 (i.e., the nearest sensor to the fault according to the smallest magnitude of the transient signals observed by the sensors) include points A and B. Then we need to decide whether the fault is more of an LSF type at point A or more of an ICF type at point B. We plug the calculated value of x back into (5) and use the plus sign corresponding to an LSF and the minus sign corresponding to an ICF to calculate the values of y, respectively. Then we compare the calculated values of y with the detected values y_i using the root-mean-square error (RMSE) in both LSF and ICF cases. For example,

$$\text{RMSE} = \left[\sum_{i=1}^{n}(y - y_1)^2/n\right]^{\frac{1}{2}}. \tag{6}$$

The case with a smaller RMSE has a higher ranking than the case with a larger RMSE so that we are able to decide which estimated fault location has a higher possibility to be close to the actual fault location.

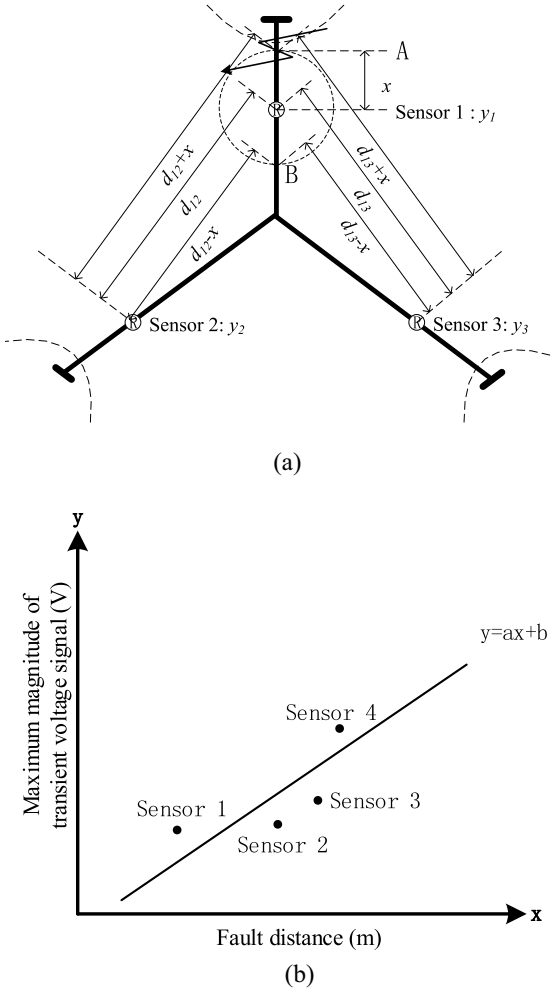

Fig. 6. (a) Schematic of fault location. (b) Coefficients calibration of a and b, where x is the fault distance, y is maximum magnitude of transient voltage signal, and a and b are confidents to be calibrated.

There exists research (see [22]) to detect the faulty zone based on information provided by protective relays, which might help reduce the number of candidate locations in this step by removing candidate location(s) not in the faulty zone.

C. Coefficient Calibration

After the fault location is found, the actual fault distance and magnitude can be visualized along with history data in

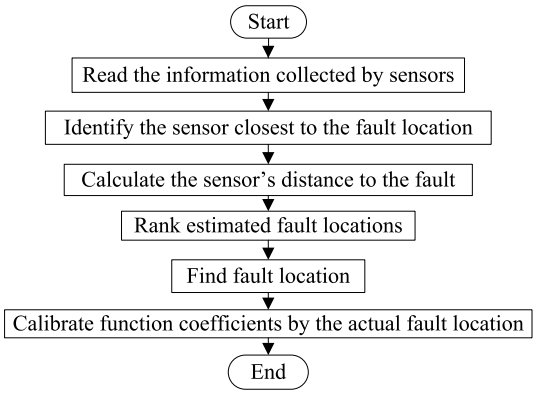

Fig. 7. Flow chart of the algorithm.

the coordinate system as illustrated in Fig. 6(b) and a new line of (2) can be computed that minimizes the fitting error, e.g., using the least square approach. Thus, the function coefficients a and b in (2) get calibrated in every fault case which may help (2) reflect the characteristics of the microgrid more and more accurately.

Although the accurate values of the coefficients a and b are unknown at the first time of fault occurrence, they can be estimated roughly by simulations of the microgrid. For example, as simulation results of a microgrid listed in Table II in the next section we can set $a = 0.001$ and $b = 0.1$ by their corresponding order.

The fault location algorithm's flow chart for one round of fault location is summarized in Fig. 7.

V. Simulation and Result Analysis

A. Simulation Design

We use EMTP for power system simulations and MATLAB for analyzing and processing data. The simulation of short circuit faults is conducted for a typical microgrid [12] whose topology is shown in Fig. 1. Referring to what has been done in [10] and [12], we set all the generators be represented by stable voltage sources. The external grid has a smaller source impedance compared with those DGs. The short circuit situation is simulated by a grounded switch and the grounded impedance is represented by the resistor, inductor, and capacitor in series and parallel. Simulations and analyses are performed corresponding to different short circuit positions in the microgrid.

The circuit line is simulated based on the distributed parameter model. We apply two parameter sets (A and B) in the simulations. The resistances, inductances, and capacitances per unit length of transmission line in set A are R1 $= 0.2\ \Omega$/km, $L1 = 0.004$ H/km, and C1 $= 5.7\ \mu$F/km. For the set B: R2 $=$ $0.1\ \Omega$/km, L2 $= 0.002$ H/km, and C2 $= 2.85\ \mu$F/km. The frequency is 60 Hz and the internal impedance of external grid and DGs are 0.5+0.43j and 1+0.86j Ohms, respectively. The loads 1–3 are all 100+0.01j Ohms while the load 4 is 200+0.01j Ohms. The short circuit lasts 0.91 ms by default at time 0.02 s and the total simulation time is 0.04 s. The ground impedance is 0.01+0.0048j Ohms.

We also conduct simulation using another microgrid topology (microgrid B) depicted in Fig. 8.

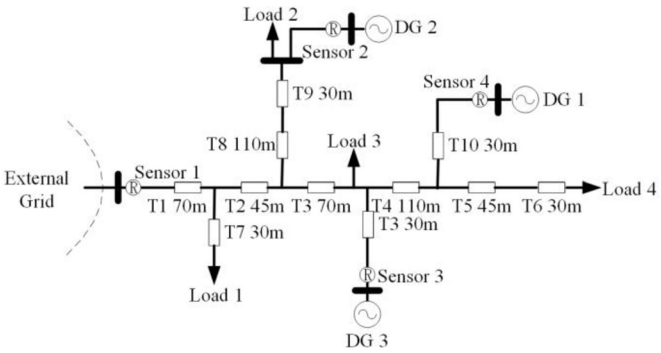

Fig. 8. Simulation topology, microgrid B.

The four cases reported here are listed below.

1) *Case 1:* Microgrid A (Fig. 1), 220 V, parameter set A.
2) *Case 2:* Microgrid A (Fig. 1), 110 V, parameter set A.
3) *Case 3:* Microgrid B (Fig. 8), 110 V, parameter set A.
4) *Case 4:* Microgrid A (Fig. 1), 110 V, parameter set B.

B. Main Simulation Results

The simulation results in this section contain two parts. The first part demonstrates the linear relationship (2) between the magnitude of the transient signal and the fault distance. The second part shows the algorithm and its performance.

To explore the internal characteristics of the microgrid, the short circuit is tested on the microgrid every 10 m. Then the data collected by EMTP would be analyzed via MATLAB.

The result of the relationship between the fault distance and the maximum magnitude of transient signal has been plotted in Fig. 9(a)–(d), where x-axis shows the fault distance and y-axis shows the maximum magnitude of transient signal. The data are collected by all sensors including sensor 1 deployed in the microgrid simulated.

Using the curve fitting toolbox of MATLAB to fit the data with candidate curves, we have observed that overall the linear function enjoys smaller RMSE than the exponential as shown in Table I. This result matches our theoretical study.

We have also observed that the coefficients in the function are proportional to the voltage level as shown in Fig. 9(a) and (b): they have the same performance except the magnitude. They are also affected by both line parameters and the microgrid topology. In the second part of simulation results, case 2 listed above is used as an example to demonstrate the algorithm and its analysis.

When a fault occurs at T2 in the microgrid of Fig. 1, i.e., 30 m away from sensor 1, the maximum magnitude of oscillating voltage signals detected by each sensor is shown in Table II. It can be seen that the sensor installed at the interface of external gird gets the minimum magnitude. Therefore, we assume that the fault position is x meters away from this sensor. Then, the distance between the fault and other sensors can also be expressed with x.

Based on the discussions in Section II and the data from Table II, we obtain the functions equations

$$\begin{cases} 0.1674 = a \cdot x + b \\ 0.2872 = a \cdot (145 - x) + b \\ 0.4468 = a \cdot (150 - x) + b \\ 0.5111 = a \cdot (270 - x) + b. \end{cases} \tag{7}$$

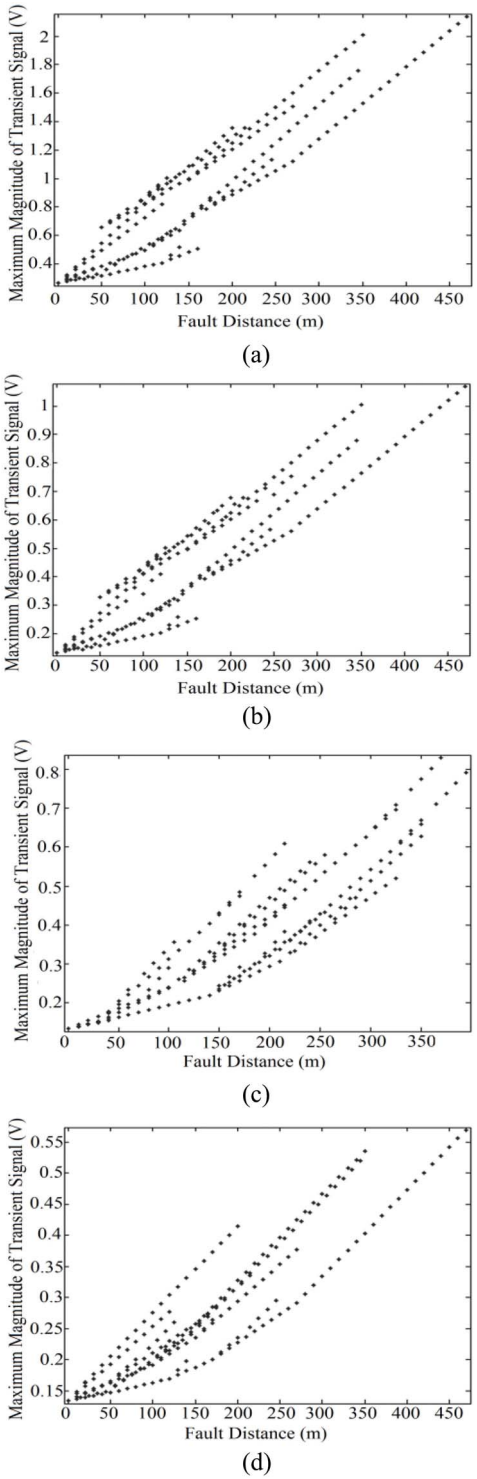

Fig. 9. Relation between transient signal magnitude and fault distance. (a) 220 V microgrid with topology *A* and parameter set *A* (case 1). 110 V microgrid with (b) topology *A* and parameter set *A* (case 2), (c) topology *B* and parameter set *A* (case 3), and (d) topology *A* and parameter set *B* (case 4).

These equations are over-determined and the specific solution can be found by the left division method: x equals 39.37 m. Based on the values of x, a, and b, the RMSE of the calculated transient voltage magnitude and the measure magnitude will be 0.3095 V if the fault is assumed to be an ICF. If we assume an LSF, then the RMSE is 0.1895 V.

TABLE I
CURVE FITTING RESULTS

	Exponential $y=a\cdot exp(b*x)$	RMSE	Linear $y=a\cdot x+b$	RMSE
Case 1	a=0.4909 b=0.00349	0.207	a=0.004105 b=0.2575	0.161
Case 2	a=0.2455 b=0.003489	0.104	a=0.002052 b=0.1288	0.086
Case 3	a=0.186 b=0.004032	0.065	a=0.001548 b=0.09403	0.066
Case 4	a=0.1617 b=0.002909	0.044	a=0.000925 b=0.1222	0.041

TABLE II
RELATION BETWEEN FAULT DISTANCE AND MAGNITUDE OF TRANSIENT VOLTAGE SIGNAL

Sensor	Sensor 1	Sensor 2	Sensor 3	Sensor 4
Magnitude (V)	0.1674 (30 m)	0.2872 (115 m)	0.4468 (120 m)	0.5111 (240 m)
Distance (m)	x	$145\pm x$	$150\pm x$	$270\pm x$

Theoretically, a smaller RMSE value means that it is closer to the real situation. In this example, however, due to the impact of the initial value setting of the unknown factors a and b, the ranking result for the first fault occurrence of this time is not correct. When the actual fault location is found, the values of a and b in (5) will be calibrated. In this case, $a = 0.0016$ and $b = 0.15$. When faults occur in the second time and later, the ranking results will become more and more accurate with the calibrated coefficients. Table III shows a series of fault location results when it is an ICF at the first time. Table IV shows the situation when it is an LSF at the first time.

It can be seen clearly from the algorithm results that, except for the ICF at the first time, the ranking results find the correct fault type, ICF or LSF. Meanwhile, there is a tiny difference between the calculated distance and the real distance. In the following section, we focus on the error analysis of this method.

C. Error Analysis

Fault location errors are calculated by (8), which has also been used in other research such as [10]. For each case listed in Section V-A, we have tested 260 fault locations and calculated the mean value of the fault location estimation errors as shown in (9). The error results are listed in Table V showing an average error in the range between 7% and 9%

$$\text{Error} = (L_{\text{Est}} - L_{\text{Act}})/L_{\text{Tol}} \cdot 100\% \tag{8}$$

$$\text{Error} = \text{Mean}(|L_{\text{Est}} - L_{\text{Act}}|)/L_{\text{Tol}} \cdot 100\% \tag{9}$$

where L_{Est} is the estimated fault location, L_{Act} is the actual fault location, and L_{Tol} is the length of total section.

In order to reduce the error, following actions might be considered:

1) building up a more sophisticated model with more accurate parameters;
2) increasing the number of sensors and using sensors with a high sampling rate and resolution.

TABLE III
FAULT LOCATION RESULTS WITH ICF IN THE FIRST TIME

Fault occurrence (Fault type)	Actual fault location	Calculated/Estimated fault location	Ranking result (RMSE)	Calibration of coefficients *a* and *b*
First time (ICF)	30 m (away from Sensor 1, ICF)	39.37 m	1. LSF (0.1895) 2. ICF (0.3095)	*a*= 0.0016 *b*=0.15
Second time (ICF)	25 m (away from Sensor 4, ICF)	22.52 m	1. ICF (0.1253) 2. LSF (0.1646)	*a*= 0.0017 *b*=0.16
Third time (LSF)	10 m (away from Sensor 3, LSF)	9.23 m	1. LSF (0.2062) 2. ICF (0.2207)	*a*=0.0017 *b*=0.17

TABLE IV
FAULT LOCATION RESULTS WITH LSF IN THE FIRST TIME

Fault occurrence (Fault type)	Actual fault location	Calculated/Estimated fault location	Ranking result (RMSE)	Calibration of coefficients *a* and *b*
First time (LSF)	50 m (away from Sensor 1, LSF)	41.40 m	1. LSF (0.4918) 2. ICF (0.6200)	*a*= 0.0016 *b*=0.22
Second time (LSF)	20 m (away from Sensor 4, LSF)	16.52 m	1. LSF (0.1493) 2. ICF (0.2189)	*a*= 0.0016 *b*=0.18
Third time (ICF)	30 m (away from Sensor 2, ICF)	32.87	1. ICF (0.0140) 2. LSF (0.2263)	*a*=0.0019 *b*=0.15

TABLE V
ERROR ANALYSIS RESULTS

	Mean error distance (m)	Line Length (m)	Error
Case 1	35.7369	470	7.6%
Case 2	35.1365	470	7.48%
Case 3	34.3152	395	8.69%
Case 4	33.8493	470	7.2%

TABLE VI
FAULT LOCATION RESULTS VERSUS LOAD FLUCTUATIONS

Load fluctuation (%): Increasing (+) or decreasing (-) of Load 2	Fault location estimation result x_{fluc} (note that the true value, denoted x_{true}, is 30m from Sensor 1)	Error fluctuation (%) corresponding to the load fluctuation: $(x_{fluc}-x_{base})/(x_{base}-x_{true})$
0% (no fluctuation)	baseline result 35.51m (denoted x_{base})	0%
+10%	35.78m	4.9%
+20%	35.74m	4.1%
+30%	36.11m	10.8%
-10%	35.56m	0.9%
-20%	36.00m	8.9%
-30%	36.21m	12.5%

D. Robustness of the Proposed Algorithm

As the load fluctuations may introduce some noise and influence the transient signal detected, we have conducted simulations under load fluctuation conditions to evaluate the robustness of the proposed fault location method. Table VI describes six scenarios of error versus load fluctuation. The short-circuit fault occurs 30 m away from sensor 1 at T2 in case 4 (i.e., microgrid *A* shown in Fig. 1 with 110 V and parameter set *B*). The fault location estimation results under six different load fluctuation conditions are illustrated in the table. Here we only have load 2 fluctuated and the other three loads are fixed. As load 2 is not in the branch where the fault occurs, it is not isolated by the fault and its fluctuation should have some impact on the sensor readings and thus the fault location estimation results. The results show the robustness of our approach in these scenarios that the fault location estimation error only changes around 10% when the load fluctuates ±30% during the fault occurrence.

TABLE VII
SENSITIVITY STUDY OF CASE 1 (TOTAL LENGTH: 470 m)

Voltage Resolution	Mean error distance (m)	Error
10^{-3}	35.7301	7.60%
10^{-2}	35.7044	7.60%
10^{-1}	36.1505	7.69%

TABLE VIII
SENSITIVITY STUDY OF CASE 2 (TOTAL LENGTH: 470 m)

Voltage Resolution	Mean error distance (m)	Error
10^{-3}	35.1514	7.48%
10^{-2}	35.1635	7.48%
10^{-1}	36.9693	7.87%

We have also simulated a high fault impedances (HIFs) case. It shows that our algorithm is still valid but would need high-resolution voltage samples to yield accurate fault location results. For example, the simulation of high ground impedances of 20+0.26j Ohms has been tested in case 1, and we observe that the linear model is still valid but the voltage differences among various fault positions become 1 mV. As HIF cases may happen in microgrids [24], [25] for ship, space station, military base, island, and mission-critical scenarios, or when the lines are buried underground or implanted in the structure, there is a need in the future research to investigate new methods for HIF cases without the need of obtaining high-resolution voltage samples.

E. Sensitivity Analysis

Sensitivity studies have been conducted to investigate how the performance of the proposed fault location method is influenced by the sample resolution of voltage sensor. As the error performance results described in Table V is based on a voltage sample resolution of 10^{-4} V, the resolution of voltage sensor used in this section is, respectively, set as 10^{-3}, 10^{-2}, and 10^{-1} V and the corresponding error performance results are shown in Tables VII–X for the four cases studied previously (cases 1–4 defined in Section V-A). The mean error

TABLE IX
SENSITIVITY STUDY OF CASE 3 (TOTAL LENGTH: 395 m)

Voltage Resolution	Mean error distance (m)	Error
10^{-3}	35.6139	9.02%
10^{-2}	35.6000	9.01%
10^{-1}	38.5444	9.76%

TABLE X
SENSITIVITY STUDY OF CASE 4 (TOTAL LENGTH: 470 m)

Voltage Resolution	Mean error distance (m)	Error
10^{-3}	34.6613	7.37%
10^{-2}	34.7208	7.39%
10^{-1}	46.2032	9.83%

distance is calculated with four digits after the decimal point for a better comparison to the results in Table V. We have observed that the voltage sample resolution does influence the error performance of the proposed method in this paper while using the relative coarse resolution (e.g., 10^{-3}, 10^{-2}, or 10^{-1} V) achieves similar error performances (e.g., $<10\%$) as those using voltage sensors with a resolution of 10^{-4} V.

VI. CONCLUSION

Microgrid has drawn increasing attention in recent years while there is little research on fault location solutions for single-phase microgrids. The difference between a single-phase microgrid and other transmission, distribution, and three-phase microgrids makes its fault location problem challenging. This paper has contributed a novel solution for fault location in single-phase microgrids.

A feature specific to the fault location for locating a fault has been revealed, which is the approximated linear relation between the magnitude of transient signals induced by the fault observed by a sensor and the distance between the sensor and the fault location. The longer the distance between the sensor and the fault location, the larger the magnitude of the transient signals sensed.

After validating this feature through extensive simulations and theoretical studies, an algorithm for fault location based on the newly discovered relationship and information fusion from multiple sensors has been designed.

Finally, the performance of the algorithm has been evaluated, including its error analysis, robustness analysis, and sensitivity analysis. The average localization error obtained is less than 10%, which should satisfy the requirement of microgrid engineering practice and manifest the significance of the novel method for solving this challenging problem.

Further research includes testing this method in field or on a test bed for single-phase microgrids with either centralized or decentralized control schemes. Future work also includes developing a software module based on this new method that can be integrated with energy management systems for microgrids.

ACKNOWLEDGMENT

The authors would like to thank K. S. Sedzro and H. Yang and anonymous reviewers for their valuable comments to improve the quality of this paper. Any opinions, findings, and conclusions expressed in this paper are those of the authors and do not necessarily reflect the views of the sponsors of the research.

REFERENCES

[1] S. Bossart, "DOE perspective on microgrids," in *Proc. Adv. Microgrid Concepts Technol. Workshop*, pp. 1–18, 2012.
[2] B. S. Hartono, Y. Budiyanto, and R. Setiabudy, "Review of microgrid technology," in *Proc. Int. Conf. QiR*, Yogyakarta, Indonesia, Jun. 2013, pp. 127–132.
[3] S. Gopalan, V. Sreeram, and H. Iu, "An improved protection strategy for microgrids," in *Proc. 4th IEEE PES Innov. Smart Grid Technol. Eur. (ISGT EUROPE)*, Lyngby, Denmark, Oct. 2013, pp. 1–5.
[4] R. Majumder, A. Ghosh, G. Ledwith, and F. Zare, "Operation and control of single phase micro-sources in a utility connected grid," in *Proc. IEEE Power Energy Soc. Gen. Meeting*, Calgary, AB, Canada, Jul. 2009, pp. 1–7.
[5] A. Khamis, A. Mohamed, H. Shareef, A. Ayob, and M. S. M. Aras, "Modelling and simulation of a single phase grid connected using photovoltaic and battery based power generation," in *Proc. Eur. Model. Symp. (EMS)*, Manchester, U.K., Nov. 2013, pp. 391–395.
[6] P. Jafarian and M. Sanaye-Pasand, "A traveling-wave-based protection technique using wavelet/PCA analysis," *IEEE Trans. Power Del.*, vol. 25, no. 2, pp. 588–599, Apr. 2010.
[7] G. B. Ancell and N. C. Pahalawaththa, "Maximum likelihood estimation of fault location on transmission lines using travelling waves," *IEEE Trans. Power Del.*, vol. 9, no. 2, pp. 680–689, Apr. 1994.
[8] IEEE guide for determining fault location on AC transmission and distribution lines, *IEEE Standard C37.114-2004*, pp. 1–36, Jun. 2005.
[9] F. H. Magnago and A. Abur, "A new fault location technique for radial distribution systems based on high frequency signals," in *Proc. Power Eng. Soc. Summer Meeting*, vol. 1. Edmonton, AB, Canada, Jul. 1999, pp. 426–431.
[10] A. Borghetti, S. Corsi, and C. A. Nucci, "On the use of continuous-wavelet transform for fault location in distribution power systems," in *Proc. Int. Conf. Elect. Power Energy Syst.*, 2011, pp. 136–142.
[11] F. H. Magnago and A. Abur, "Fault location using wavelet packets," *IEEE Trans. Power Del.*, vol. 13, no. 4, pp. 2575–2579, Oct. 1998.
[12] S. M. Brahma, "Fault location in power distribution system with penetration of distributed generation," *IEEE Trans. Power Del.*, vol. 26, no. 3, pp. 1545–1553, Jul. 2011.
[13] L. A. C. Lopes and S. Huili, "Performance assessment of active frequency drifting islanding detection methods," *IEEE Trans. Energy Convers.*, vol. 21, no. 1, pp. 171–180, Mar. 2006.
[14] G. K. Hung, C. C. Chang, and C. L. Chen, "Automatic phase-shift method for islanding detection of grid connected photovoltaic inverters," *IEEE Trans. Energy Convers.*, vol. 18, no. 1, pp. 169–173, Mar. 2003.
[15] M. Ropp, J. Ginn, J. Stevens, W. Bower, and S. Gonzalez, "Simulation and experimental study of the impedance detection anti-islanding method in the single-inverter case," in *Proc. IEEE Photovolt. Energy Convers. Conf.*, vol. 2. Waikoloa, HI, USA, May 2006, pp. 2379–2382.
[16] G. Hernandez-Gonzalez and R. Iravani, "Current injection for active islanding detection of electronically-interfaced distributed resources," *IEEE Trans. Power Del.*, vol. 21, no. 3, pp. 1698–1705, Jul. 2006.
[17] E. Casagrande, W. L. Woon, H. H. Zeineldin, and N. H. Kan'an, "Data mining approach to fault detection for isolated inverter-based microgrids," *IET Proc. Gener. Transm. Distrib.*, vol. 7, no. 7, pp. 745–754, Jul. 2013.
[18] S. A. Saleh, R. Ahshan, M. A. Rahman, M. S. A. Khaizaran, and B. Alsayed, "Implementing and testing *d–q* WPT-based digital protection for microgrid systems," in *Proc. Ind. Appl. Soc. Annu. Meeting*, Orlando, FL, USA, Oct. 2011, pp. 1–8.
[19] T. Basso and R. DeBlasio, "IEEE smart grid series of standards IEEE 2030 (interoperability) and IEEE 1547 (interconnection) status," in *Proc. Innov. Smart Grid Technol. (ISGT)*, Washington, DC, USA, Jan. 2012, pp. 1–7.
[20] A. G. Tsikalakis and N. D. Hatziargyriou, "Centralized control for optimizing microgrids operation," *IEEE Trans. Energy Convers.*, vol. 23, no. 1, pp. 241–248, Mar. 2008.
[21] A. Greenwood, *Electrical Transients in Power Systems*, 2nd ed. Hoboken, NJ, USA: Wiley, 1991, pp. 37–46.

[22] H. Al-Nasseri and M. A. Redfern, "Harmonics content based protection scheme for micro-grids dominated by solid state converters," in *Proc. Int. Middle-East Power Syst. Conf.*, Aswan, Egypt, Mar. 2008, pp. 50–56.
[23] J. Park, J. Candelaria, M. Liuyan, and K. Dunn, "DC ring-bus microgrid fault protection and identification of fault location," *IEEE Trans. Power Syst.*, vol. 28, no. 4, pp. 2574–2584, Oct. 2013.
[24] E. Sortomme, S. S. Venkata, and J. Mitra, "Microgrid protection using communication-assisted digital relays," *IEEE Trans. Power Del.*, vol. 25, no. 4, pp. 2789–2796, Oct. 2010.
[25] Q. Li, Z. Xu, and L. Yang, "Recent advancements on the development of microgrids," *J. Mod. Power Syst. Clean Energy*, vol. 2, no. 3, pp. 206–211, Sep. 2014.

Jiajun Duan (S'14) was born in Gansu, China, in 1990. He received the B.S. degree from Sichuan University, Chengdu, China, in 2013, and he is currently pursuing the M.S. degree with Lehigh University, Bethlehem, PA, USA, both in electrical engineering.

His current research interests include power system analysis, power electronics, control systems, renewable energy, and smart grid.

Kaifeng Zhang (M'10) received the Ph.D. degree in power system and its automation from Southeast University, Nanjing, China, in 2004.

He joined the faculty of Southeast University, where he is currently a Professor. He is a Visiting Scholar with Lehigh University, Bethlehem, PA, USA. His current research interests include power system modeling, control and dispatch, power market, and microgrids.

Liang Cheng (S'01–M'03) received the Ph.D. degree in electrical and computer engineering from Rutgers, State University of New Jersey, New Brunswick, NJ, USA, in 2002.

He is an Associate Professor with Lehigh University, Bethlehem, PA, USA. He has advised six Ph.D. students to their graduation and two postdoctoral researchers. He was the Principal Investigator (PI) and the Co-PI of 15 projects supported by the U.S. National Science Foundation, the Defense Advanced Research Projects Agency, the Department of Energy, and state and industry sponsors. His current research interests include ad-hoc/sensory networks and system instrumentation/analytics.